Differential Inelastic Scattering Cross-Section of Silicon and Gallium Arsenide Semiconductor Crystals

H. Kabil[1], E. Sakar[2,*], A. Meral[1], M. Sahin[1] and A. Gürol[2]

[1]Department of Physics, Faculty of Arts and Sciences, Recep Tayyip Erdogan University, 53100 Rize, Turkey
[2]Department of Physics, Faculty of Science, Atatürk University, 25240 Erzurum, Turkey

*Corresponding author: Fax: +90 442 2314143; Tel: +90 442 2314172; E-mail: erdem@atauni.edu.tr

Because of the extensive usage of silicon and gallium arsenide semiconductor crystals, the differential inelastic scattering cross-sections at 59.5 keV have been measured for various scattering angles changing from 120 to 150 degrees by using an energy dispersive X-ray fluorescence spectrometer. The spectrometer includes an Am-241 radio isotopes as photon source and a Si(Li) detector. Experimental results of differential inelastic scattering cross-sections compared with theoretical results. We found a good agreement between experimental and theoretical values in the standard uncertainties. To our best of knowledge, these results are first data in the differential inelastic scattering cross-sections of silicon and gallium arsenide crystals.

Keywords: Differential inelastic scattering cross sections, Semiconductors, Crystal structure.

INTRODUCTION

If a photon interacts with a matter it can be carried out different interactions between it and electrons in the matter (or nuclei and coulomb fields surrounding them). Although there is a long list of possible interactions, when the photon energy is below 1 MeV, the major interaction processes are considered as the atomic photoelectric absorption, Inelastic (Compton) scattering and Rayleigh scattering [1]. The Compton scattering is a collision between a photon and a so-called free and rest electron. But all the electrons in the matter are not free. If the energy of incident photon is higher than binding energy of the electron, this electron may be considered free [2]. The probability of any event occurring depends on the energy of the incident photon and a cross-section dealing with any event is described as a measure of this probability. Compton scattering cross-section of free electron is described by the Klein-Nishina formula. In this formula, the electron binding effect is negligible and the Compton scattering must be treated as scattering by a free electron. In real atoms the electrons are neither free nor at rest. For this reason, an adjustment term is required for the accurate results. This term is called as a incoherent scattering function S(q,Z) in which q is a momentum transfer variable and Z is the atomic number of the target. Momentum transfer variable q depends on the incident photon energy and the scattering angle [1].

In the Compton scattering, the relationship between the energies of incident and scattered photons, E_i and E_s, are given by following equation:

$$E_s = \frac{E_i}{1 + \frac{E_i}{m_0 c^2}(1 - \cos\theta)} \qquad (1)$$

where the $m_0 c^2$ is the rest mass energy of the electron and θ is the scattering angle which is between the directions of the incident and the scattered photons.

The Compton scattering differential cross section per atom can be theoretically calculated by using the following relation given by Hubbell *et al.* [3].

$$\frac{d\sigma_c}{d\Omega} = \frac{d\sigma_{KN}}{d\Omega} S(q,Z) \qquad (2)$$

where, $d\sigma_{KN}/d\Omega$ is the Klein-Nishina prediction for the Compton scattering cross section at the same angle per electron assumed free and at rest Klein and Nishina [4].

$$\frac{d\sigma_{KN}}{d\Omega} = \frac{r_e^2}{2}\left[1 + k(1 - \cos\theta)\right]^{-2}\left[1 + \cos^2\theta + \frac{k^2(1 - \cos\theta)^2}{1 + k(1 - \cos\theta)}\right] \qquad (3)$$

where, r_e is the classical electron radius and k is the photon energy in units of the electron rest-mass energy. The momentum transfer variable q is given by

$$q = \sin(\theta/2)/\lambda \text{ (Å)} \qquad (4)$$

where λ is the wavelength. In order to calculate the incoherent-scattering function S(q,Z), different models have been used. The most widely used models are Thomas-Fermi and Hartree-Fock models [5-7].

Accurate determination of ratios of differential inelastic scattering cross-sections for different materials is important because of their use in the fields of atomic physics, reactor shielding, industrial radiography, space physics and chemistry, dosimetry, environmental production and material analysis by various techniques [8-11]. While the coherent scattering measurements are used for Z-dependent characterization of materials the incoherent scattering measurements are generally preferred to determine the electron-momentum densities [12-15].

n-Type gallium arsenide (GaAs) sample has a zinc blend structure and lattice constant is 5.653 Å. Band gap (E_g) at 300 K is 1.43 eV and it has a direct band transition. It has 4.42×10^{22} molecule per volume (cm^{-3}). n-Type GaAs sample acquired by doping chrome (Cr) and oxygen (O) to GaAs and is direction is (100). n-Type silicon (Si) sample has a diamond structure and lattice constant 5.430 Å and its direction is (100). The energy gap at 300 K is about 1.11 eV. There are 5.0×10^{22} atoms per volume (cm^{-3}) and it has doped phosphor (P) about 10^{14} order.

GaAs and Si semiconductor crystals are considered as technologically important materials because of their usage for high speed microelectronics and optoelectronic applications *i.e.,* microwave frequency integrated circuits, light-emitting diodes, laser diodes and solar cells. Furthermore, these crystals are used to detect the X-ray and γ-ray radiations. Because of the extensive usage of GaAs and Si, in the present work we have measured incoherent scattering differential cross-sections for Si and GaAs semiconductor crystals at 59.5 keV using Si(Li) detector.

EXPERIMENTAL

The experimental setup of the energy dispersive X-ray fluorescence (EDXRF) spectrometer is shown in Fig. 1. We used a point ^{241}Am radioisotope source with ~3.7 GBq activity for photon source. The scattered photons from the Si and GaAs crystals were recorded by using a Si(Li) detector (full-width at half- FWHM ~160 eV at 5.9 keV, active diameter 3.91 mm, active area 12 mm^2, sensitivity depth 3 mm and Be window thickness 0.025 mm). The detector has been shielded with Pb, Fe and Al metals. The Pb shield has been used to avoid direct exposure of the detector from the radiation source. The Fe and Al shields located inside of Pb shields have been used to absorb the Pb L X-rays and Fe K X-rays, respectively. The recorded spectrum was recorded using Genie 2000 VDM Software. A typical Compton scattering spectrum of Si crystal is shown in Fig. 2.

The differential cross section was determined by using

$$\frac{d\sigma_c}{d\Omega} = \frac{N_c}{4\pi \, I_0 G \varepsilon_c \beta_c t} \tag{5}$$

where N_c is the number of counts per unit time under the Compton scattering of 59.5 keV γ-ray peak, I_0 is the intensity of incident radiation, G is a geometrical factor, ε_c is the detector efficiency at the energy of Compton scattered 59.5 keV γ-ray
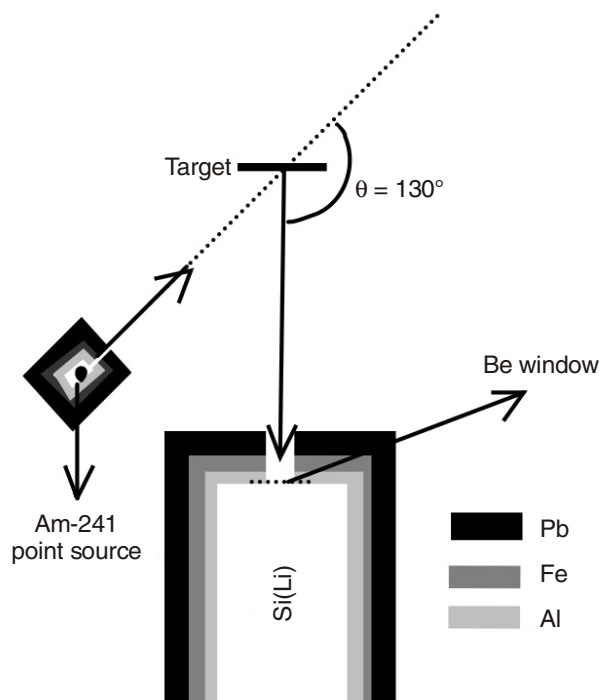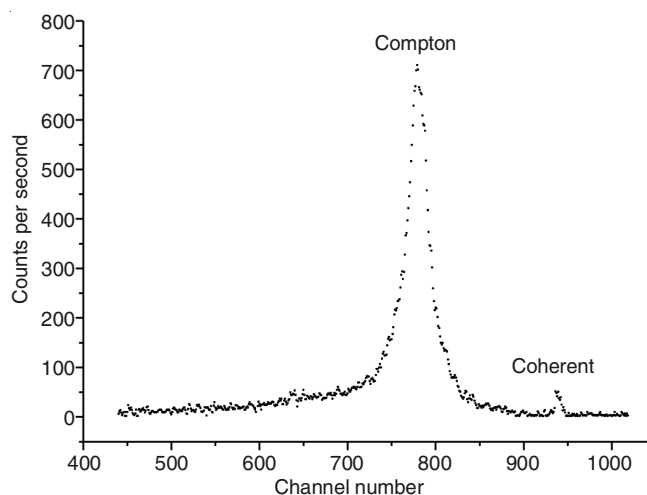

Fig. 1. Experimental setup used in the experiments

Fig. 2. Typical scattering spectrum of γ-rays from silicon crystal measured at 130°. It is shown the elastic and inelastic (Compton) scattering peaks in the spectrum

and β_c is the self-absorption correction factor for the target material, t is the thickness (g cm^{-2}) of the sample. The values of β_c have been calculated by using the following equation:

$$\beta_c = \frac{1 - \exp\left[-\left(\mu_1 / \cos\phi_1 + \mu_2 / \cos\phi_2\right) t\right]}{\left(\mu_1 / \cos\phi_1 + \mu_2 / \cos\phi_2\right) t} \tag{6}$$

where μ_1 and μ_2 are the attenuation coefficients (cm^2/g) of incident and scattering photons, respectively. μ_1 and μ_2 were obtained from the table of Hubbell and Seltzer [16]. ϕ_1 and ϕ_2 are the angle of incident photons and scattered γ-rays with respect to the normal at the surface of the sample in the present setup, respectively. In this study, the value of the factor $I_0 G \varepsilon_c$ which contain terms related to the incident photon flux, geometrical factor and the efficiency of the γ-ray detector was determined by measuring K_α X-ray intensities from thin

samples of Pd, Ag, Cd, Sn, Te, Sm and Dy in same geometry. $I_oG\varepsilon$ values were determined by using:

$$I_oG\varepsilon_c = \frac{N_{K_\alpha}}{\sigma_{K_\alpha}\beta_{K_\alpha}t} \qquad (7)$$

where the various terms are similar in eqn. 5 whereas σ_{K_α} is the K_α X-ray production cross section of target. The theoretical $K\alpha$ X-ray production cross sections σ_{K_α} were calculated by using the fundamental parameter equation:

$$\sigma_{K\alpha} = \sigma_K(E)\omega_K F_{K_\alpha} \qquad (8)$$

where $\sigma_K(E)$ is the K shell photoionization cross section for the given elements at excitation energy E, ω_K is the fluorescence yields of the K-shell. In the present calculations, the values of $\sigma_K(E)$ were taken from table of Scofield [17] and the values of were taken from an annotated bibliography [18]. The value is the fractional ratio of the K_α X-rays. These ratios were taken from the table published by Scofield [19].

RESULTS AND DISCUSSION

The measurements of GaAs and Si samples were carried out at different angles, from 120° to 150° with 5° intervals. To obtain the areas of Compton peaks, we have firstly fitted a polynomial background to each spectrum and then we have subtracted the background from raw data and we lastly have determined the peak areas. The inelastic differential cross-sections of Si and GaAs crystals calculated by using eqn. 5 are presented in Table-1 (Fig. 3). There is a good agreement between present experimental and theoretical values for Si. But there is a small disagreement for GaAs crystal. It is presumed that the possible source of the disagreement is arisen from the chemical effects in GaAs crystal, *i.e.* the energy of the valance electrons of GaAS crystal increase due to the chemical bonds and the inelastic Compton scattering cross-sections decrease. Moreover, the theoretical cross-sections are generally higher then experimental values.

TABLE-1
EXPERIMENTAL AND THEORETICAL VALUES
OF INELASTIC CROSS SECTIONS (barns/atom)

Angle (°)	Si		GaAs	
	Exp.	Theo.	Exp.	Theo.
120	0.511 ± 0.048	0.510	1.130 ± 0.0565	1.18
125	0.527 ± 0.049	0.534	1.120 ± 0.0560	1.18
130	0.567 ± 0.051	0.561	1.150 ± 0.0575	1.13
135	0.579 ± 0.052	0.583	1.230 ± 0.0615	1.21
140	0.629 ± 0.056	0.618	1.340 ± 0.0671	1.37
145	0.651 ± 0.058	0.644	1.390 ± 0.0696	1.43
150	0.667 ± 0.060	0.669	1.420 ± 0.0712	1.48

The overall errors in the present measurements of inelastic scattering differential cross sections are estimated to be 4-5 %. The errors are based on the uncertainties in the different parameters used to evaluate the inelastic scattering differential cross sections, namely, the evaluation of peak areas (~2-3 %), target thickness measurement (~1 %), $I_oG\varepsilon_c$ factors (~3 %) and absorption correction factor (~2 %).

In a crystal, Compton scattering mostly happened with conductivity electrons that can be considered as free electrons.
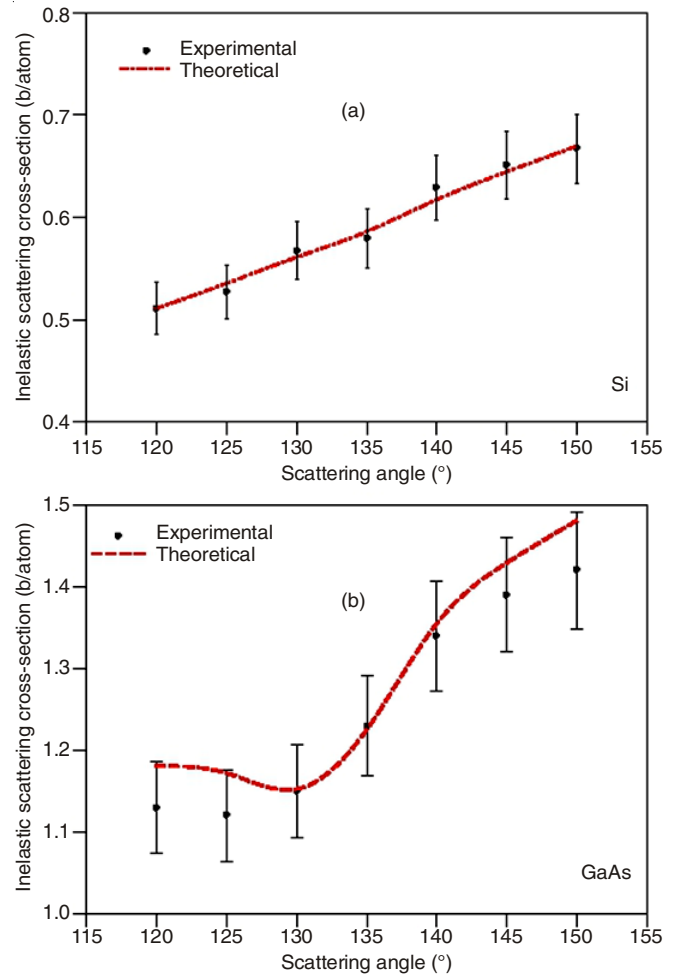

Fig. 3.   Differential inelastic scattering cross-sections *versus* scattering angle (a) for silicon (b) for gallium arsenide

However, this scattering can be also happen at inner shells. The conductivity electrons of atoms in a crystal have less bonding energy than the electrons of a free atom. Because of this, the scattered photon numbers increase in a crystal. As a result, the Compton peaks measured from a crystal become narrower. With these explanations, we can comment about bonding energy in crystal as explained by DuMond [20] and DuMond and Hoyt [21].

Conclusions

Our work has some limitations. First, we have neglected the scattering from doped elements. But it doesn't affect the result, because their concentrations are trace levels and scattering photon numbers are very small and their contribution to intensity can be easily neglected. Second limitation is the multiple scattering. To minimize this effect, we have got thinner samples as much as possible (~0.05 mm). Nevertheless, we haven't wholly eliminated the multiple scatterings. But, since the path length of photons in the sample are nearly same at different scattering angles it is suggested that the contributions of intensities nearly same at different angles.

Timms *et al*. [22] investigated the Compton scattering from GaAs at different directions and they found an important difference among different directions. Sahin and Demir [23] reported a decreasing of Compton scattering from a p type Si with a increasing current at a magnetic field. Despite of our

careful researches we have not found any investigation apart from these papers in the literature. To our best of knowledge, our results are first results about inelastic scattering cross-sections of Si of GaAs and someone can easily see that there is an angular dependence at inelastic scattering cross sections.

Inelastic scattering at different directions in a crystal occurs different from each other [22]. We use the crystals that only have one direction (100) and the exact understanding of the inelastic scattering from a crystal repeats the experiments with crystal having different directions. In spite of the limitations our results still are reliable, correct and precise data for inelastic scattering cross-sections of n-type Si and GaAs.

REFERENCES

1. J.H. Hubbell, *Radiat. Phys. Chem.*, **50**, 113 (1997).
2. N. Tsoulfanidis, Measurement and Detection of Radiation, Taylor & Francis, Washington, pp. 614 (1998).
3. J.H. Hubbell, W.J. Veigele, E.A. Briggs, R.T. Brown, D.T. Cromer and R.J. Howerton, *J. Phys. Chem. Ref. Data*, **4**, 471 (1975).
4. O. Klein and Y.Z. Nishina, *Z. Phys.*, **52**, 853 (1929).
5. L.H. Thomas, *Mathematical Physical Sci.*, **23**, 542 (1926).
6. E. Fermi, *Z. Phys.*, **48**, 73 (1928).
7. H. Fock, *Z. Phys.*, **61**, 126 (1930).
8. I. Han, M. Sahin, L. Demir and M. Kacal, *Balkan Phys. Lett.*, **18**, 377 (2010).
9. U. Schiebel, A. Neufert and G. Clausnitzer, *Radiat. Effects Defects Solids*, **29**, 57 (1976).
10. J. Matsumoto, F. Kwiatkowska, A. Maniawski, S. Bansil, M. Kaprzyk, H. Itou, N. Kawata and A. Shiotani, *J. Phys. Chem. Solids*, **61**, 375 (2000).
11. A. Kumar, J.S. Shahi, D. Mehta and N. Singh, *Nucl. Instr. Methods B*, **194**, 105 (2002).
12. F. Van Langevelde and R.D. Vis, *Anal. Chem.*, **63**, 2253 (1991).
13. M.F. Araújo, P. Van Espen and R. Van Grieken, *XRay Spectrom.*, **19**, 29 (1990).
14. K.K. Nielson, *Anal. Chem.*, **49**, 641 (1977).
15. J.S. Shahi, A. Kumar, D. Mehta, S. Puri, M.L. Garg and N. Singh, *Nucl. Instr. Methods B*, **179**, 15 (2001).
16. J.H. Hubbell and S.M. Seltzer, National Institute of Standards and Technology Report No. 5632 (1995).
17. J.H. Scofield, UCRL Report No. 51326, Livermore, California (1973).
18. J.H. Hubbell, P.N. Trehan, N. Singh, B. Chand, D. Mehta, M.L. Garg, R.R. Garg, S. Singh and S. Puri, *J. Phys. Chem. Ref. Data*, **23**, 339 (1994).
19. J.H. Scofield, *At. Data Nucl. Data Tables*, **14**, 121 (1974b).
20. J.W.M. DuMond, *Phys. Rev.*, **33**, 643 (1929).
21. J.W.M. DuMond and A. Hoyt, *Phys. Rev.*, **36**, 146 (1930).
22. D.N. Timms, M.J. Cooper, R.S. Holt, F. Itoh, T. Kobaysai and H. Nara, *J. Phys. Condens. Matter*, **2**, 10517 (1990).
23. Y. Sahin and D. Demir, *XRay Spectrom.*, **32**, 336 (2003).